

Simulating bipedal walking using a translating center of pressure

Karna Potwar¹ and Dongheui Lee^{1,2}

¹ Technical University of Munich (TUM)

² German Aerospace Center (DLR)

August 2, 2019

1 **Abstract**

2 During walking, foot orientation and foot placement allow humans to
3 stabilize their gait and to move forward. Consequently the upper body adapts
4 to the ground reaction force (GRF) transmitted through the feet. The foot-
5 ground contact is often modeled as a fixed pivot in bipedal models for anal-
6 ysis of locomotion. The fixed pivot models, however, cannot capture the
7 effect of shift in the pivot point from heel to toe. In this study, we propose
8 a novel bipedal model, called $SLIP_{COP}$, which employs a translating center
9 of pressure (COP) in a spring loaded inverted pendulum (SLIP) model. The
10 translating COP has two modes: one with a constant speed of translation and
11 the other as the weighted function of the GRF in the fore aft direction. We
12 use the relation between walking speed and touchdown (TD) angle as well
13 as walking speed and COP speed, from existing literature, to restrict steady
14 state solutions within the human walking domain. We find that with these
15 relations, $SLIP_{COP}$ provides steady state solutions for very slow to very fast
16 walking speeds unlike SLIP. $SLIP_{COP}$ for normal to very fast walking speed
17 shows good accuracy in estimating COM amplitude and swing stance ratio.
18 $SLIP_{COP}$ is able to estimate the distance traveled by the COP during stance
19 with high precision.

20 **1 Introduction**

21 Walking is an efficient form of locomotion which allows humans to travel from
22 one place to another. Human walking has two facets, which are reducing cost of
23 locomotion and gait stabilization. Foot placement and orientation plays an im-
24 portant role in stabilizing our gait. To improve our understanding of walking and
25 its underlying mechanism, human motion capturing and reductive modeling have
26 been widely used [1]. Human body is a complex redundant system and reductive
27 models or templates strip down the complex architecture of the body into simple
28 elements and allow a computationally inexpensive way to simulate locomotion,
29 with a certain degree of accuracy [1]. The earliest versions of such templates
30 include the sagittal plane based inverted pendulum model (IP) [2, 3] and spring-
31 mass model [4, 5]. The IP model assumes incompressible legs with center of mass
32 (COM) vaulting over the legs, with a fixed foot. Due to its rigid legs, IP model
33 provides an incorrect representation of ground reaction force (GRF) pattern, com-
34 pared to that observed in humans. To overcome this drawback of the IP model,
35 some templates include a springy leg to obtain more accurate estimates of walking
36 gait trajectories [6, 7, 8, 9, 10]. One such model is the sagittal plane based SLIP
37 model [10]. Due to SLIP's compliant legs it is able to generate the COM trajectory
38 and GRF pattern during walking to that observed in human walking. The steady

39 state solutions of SLIP also suggests that walking is one of the many domains of
40 different locomotion patterns generated. Hence, it is important to narrow down
41 the parameters in a bipedal model pertaining only to the domain of walking.

42 IP model and SLIP model assume a fixed pivot during stance as discussed
43 above, which is essentially the mean position traveled by COP during stance. In
44 a study to analyze treadmill walking¹, SLIP fairly estimates COM trajectory at
45 1m/s, while failing to estimate at other walking speeds [11]. They also men-
46 tion that due to the fixed pivot of the SLIP, the model has to be simulated at a
47 steeper TD angle compared to human walking. This characteristic of SLIP might
48 be restricting its predictive capabilities at slower and faster walking speed. During
49 walking, COP of a particular foot travels approximately a distance of a foot length
50 and the COP progression velocity depends on speed of walking [12, 13, 14]. To
51 accommodate the mechanical consequences of COP progression, a few bipedal
52 models were developed for running [15, 16] and walking [17, 18]. Bullimore et
53 al. [16] take into consideration the change in TD and LO angles caused by COP
54 translation, called POFT (point of force translation), in the conventional spring
55 mass model for running. They use a constant velocity based COP progression
56 model without considering the acceleration of the COP during stance. They ob-

¹Subjects walked at speeds of (0.52,1.04,1.55,2.07 and 2.59) m/s in this experiment

57 serve similar COM trajectories and GRF patterns as in human running but the
58 model shows drastic decrease in spring stiffness. Lee et al. [17] use a translating
59 point of force application (PFA) in an IP model for walking and show that the
60 error in vertical displacement of the COM predicted by the model increases from
61 111% to 240%, as walking speed increases from 0.5 m/s to 2.5 m/s respectively.
62 However, these errors were considerably lesser compared to IP model with a fixed
63 pivot. Miff et al. [18] show that during walking vertical excursion of the trunk is
64 dependent on the foot rocker radius in the rocker based IP model. IP models in
65 the above studies consider only the single stance vaulting of the COM but not the
66 foot impact and double stance phase of walking. We need a bipedal model which
67 can simulate COP progression along with single/double stance, COM trajectory
68 and GRF patterns.

69 The objective of this study is to check, if addition of a COP progression model
70 would improve SLIP model's performance at slower and faster walking speeds.
71 Instead of using a predefined leg stiffness [11], we optimize our spring stiffness.
72 We use the relation between TD angle, walking speed and COP speed obtained
73 from existing literature so as to make model-experiment comparison. We develop
74 a generic model called $SLIP_{COP}$ (Fig. 1) with COP progression considering two
75 modes of COP translation during stance: one with a constant COP speed and the

76 other accelerated COP. We include the constant velocity COP progression model
77 so as to compare our model with previous similar models. We make inter-model
78 comparisons between SLIP and SLIP_{COP} for various walking parameters to an-
79alyze the results qualitatively and quantitatively. Subsequently, we compare the
80 two models with real walking scenarios to assess the quality of our solutions.

81 **2 Method**

82 We simulate the two models, SLIP and SLIP_{COP}, as seen in Fig. 1. The position
83 and velocity of right and left COP are denoted as $[f_r, \dot{f}_r]$ and $[f_l, \dot{f}_l]$ respectively.
84 For SLIP, \dot{f}_r and \dot{f}_l are always 0 due to a fixed pivot. Like the conventional SLIP,
85 SLIP_{COP} consists of a COM attached with two springy legs. The legs are con-
86 sidered massless and a swinging leg can be ignored. As illustrated in Fig. 2,
87 COM state at apex is described by $[x, \dot{x}, y, \dot{y}]$ and at TD the leg makes an angle of
88 θ_o . Both models are simulated in the sagittal plane. We non-dimensionalize the
89 equations of motion to develop generic models catering to humans with different
90 anthropometric measurements [19, 20, 21]. Force experienced by the COM before
91 non-dimensionalization in the forward and vertical direction is given as

$$F_{x_d} = m\ddot{x}_d = F_{rd} \cos \alpha + F_{ld} \cos \beta \quad (1)$$

$$F_{y_d} = m\ddot{y}_d = F_{rd} \sin \alpha + F_{ld} \sin \beta - mg \quad (2)$$

where $F_{rd} = k(L_o - L_{rd})$ is the GRF in the right leg, m is the mass, k is the spring stiffness, g acceleration due to gravity, $L_{rd} = \sqrt{((x_d - f_{rd})^2 + (y_d)^2)}$ is the length of the right leg in stance, L_o is the uncompressed leg length, the subscript l and r refer left and right leg, and the subscript d means dimensionalized. Upon non-dimensionalizing eqns.(1)(2), the time-dependent terms are divided by $\sqrt{\frac{L_o}{g}}$, distance terms by uncompressed leg length L_o and divide the equations throughout by mg [20, 10]. After non-dimensionalization the force experienced by the COM is given as

$$F_x = \ddot{x} = \tilde{F}_r \cos \alpha + \tilde{F}_l \cos \beta \quad (3)$$

$$F_y = \ddot{y} = \tilde{F}_r \sin \alpha + \tilde{F}_l \sin \beta - 1 \quad (4)$$

92 where $\tilde{F}_r = \tilde{k}(1 - L_r)$ (see Fig. 1), $\tilde{k} = \frac{kL_o}{mg}$ is the relative stiffness of the legs. At
 93 TD, the leg angle reorients to θ_o and at lift off (LO) occurs when the GRF becomes
 94 0.

95 **2.1 Gait parameter relations**

In order to restrict our model's solution search within the walking domain, we use the relation between walking speed, TD angle and COP speed obtained through existing literature [11, 12] (see Table 2). The lower and upper bound for the COP progression velocity are the minimum and maximum speed of the COP during experimental walking. The COP model during stance is described as the function of the GRF in the fore-aft direction as

$$\ddot{f}_r = \mu F_r \cos \alpha \quad (5)$$

$$\ddot{f}_l = \mu F_l \cos \beta \quad (6)$$

96 Especially, two modes of this translating COP model are considered: one con-
97 sidering effect of a constant COP speed during stance ($\mu = 0$) and the other as
98 weighted function of the GRF during stance ($\mu = 1$).

99 We obtain steady state solutions of the two models by optimizing their param-
100 eters to generate a limit cycle. To generate a limit cycle we consider the apex
101 to apex state errors. The state of the model at apex is completely described by
102 its relative horizontal distance between COM and COP denoted by $(x - f)$, hor-
103 izontal velocity \dot{x}_i , apex height y_i , vertical velocity \dot{y}_i , and COP velocity \dot{f}_i . To
104 obtain a limit cycle, we calculate the stride to stride error for consecutive apex

Algorithm 1 Algorithm to obtain a limit cycle

To Optimize: $[\tilde{k}, \dot{f}_r, \dot{f}_l]$

Constraints: $5 < \tilde{k} < 80, f_{LB} < \dot{f}_r, \dot{f}_l < f_{UB}$

if SLIP **then**

fixed pivot

else if SLIP_{COP} **then**

translating pivot, $\mu = 0$ or $\mu = 1, \dot{f} > 0$

for μ **do**

for $\dot{x} = \dot{x}_{min} : \dot{x}_{max}$ **do**

Estimate $\theta_o, \dot{f}_{LB}, \dot{f}_i, \dot{f}_{UB}$ from Table. 2

for $y_o = \sin(\theta_o) : 1$ **do**

Optimize Parameters $[\tilde{k}, \dot{f}_r, \dot{f}_l]$

Solve eqns.(3)(4)(5)(6)

Evaluate error (e) between apex states

$$e = [\dot{x}_{i+1} - \dot{x}_i; x_{i+1} - f_{l(i+1)}; y_{i+1} - y_i;$$

$$\dot{y}_{i+1} - \dot{y}_i; \dot{f}_{l(i+1)} - \dot{f}_{r(i)}]$$

end for

end for

end for

end if

105 states (i and $i + 1$) using a 5-dimensional nonlinear Poincaré return map [22]. The
106 initial apex state and final apex state of the model are given as $[x, \dot{x}, y, \dot{y}, f_r, \dot{f}_r]_i$ and
107 $[x, \dot{x}, y, \dot{y}, f_l, \dot{f}_l]_{i+1}$ respectively. For a given set of $x_i, \dot{x}_i, y_i, \dot{y}_i$, we optimize relative
108 stiffness \tilde{k} , right COP speed \dot{f}_r and left COP speed \dot{f}_l to get a limit cycle as shown
109 in the Algorithm 1. At the start of simulation, the foot is placed at the origin with
110 the COM directly above it.

111 **3 Results**

112 Firstly, we compare COM, COP and GRF trajectories for the two models (SLIP,
113 $SLIP_{COP}$) for a given set of optimized parameters (see Table 1) to assess the qual-
114 itative nature of the solutions. Fig. 4a & b are GRF and COP trajectories for
115 individual legs. GRF pattern in vertical and horizontal direction resemble that of
116 experimental walking[10, 11, 23]. $SLIP_{COP}$ shows a lower vertical GRF value at
117 mid-stance (F_y), for both of the COP modalities ($\mu = 0$ and 1) compared to SLIP.
118 At $\mu = 0$ the COP translates with constant speed and at $\mu = 1$ the speed results
119 in a U-shape profile which correlates to the horizontal GRF (F_x) (Fig. 4b). The
120 shape of the COP speed trajectory for $\mu = 1$ resembles the COP speed trajectory
121 of human walking. As seen in Fig. 4c, $SLIP_{COP}$ has higher COM amplitude and

122 horizontal distance travelled than SLIP. This result, as expected, is a consequence
123 of COP progression. A higher gait distance for $\mu = 1$ is due to a larger average
124 COP speed (see Fig. 4b) compared to at $\mu = 0$.

125 We make inter-model comparisons at a non-dimensionalized speed $\dot{x}_i = 0.335$
126 and $\theta_o = 76.33^\circ$. We compare the steady state solutions, at the mentioned speed
127 and TD angle, obtained by varying $y_i \in (\sin(\theta_o), 1)$. We discard solutions at
128 $y_i = \sin(\theta_o)$ and $y_i = 1$. Because at $y_i = \sin \theta_o$ the apex height will be equal to
129 the COM height at TD, which is physically impossible. And at $y_i = 1$, the system
130 will be under free fall as the leg will be at its natural uncompressed length sug-
131 gesting no foot contact with the ground. As seen in Fig. 5a for SLIP, increase in
132 y_i leads to increase in \tilde{k} , from 22.75 to 29.54. $SLIP_{COP}$ for both COP modalities
133 shows a considerably lower and constant stiffness for all values of y_i . We ex-
134 pected lower stiffness for $SLIP_{COP}$ because of the leg lengthening that occurs due
135 to a virtual pivot point generated as shown in Fig. 3. During walking, stride length
136 is approximately twice the value of step length as seen in Fig. 5c & e. A higher
137 value for step lengths for $SLIP_{COP}$ is observed: e.g. a value of 0.46 at $y_i = 0.99$
138 with $\mu = 1$. For walking, cadence c and step length s_l are related to walking speed
139 as $v = (c)(s_l)$ [18]. We see the effect of this hyperbolic relation between cadence
140 c and step length s_l in the plots Fig. 5c & d. The swing/stance duration ratio

141 is around 0.4 for walking, and SLIP achieves this ratio as y_i approaches 1 (see
142 Fig. 5f). $SLIP_{COP}$ shows a reduced swing/stance duration time which occurs due
143 to its increased stance time. This increase in stance time occurs as a result of the
144 COP progression which we expected [16].

145 The reliability of the two models is tested by making model-experiment com-
146 parisons. In particular, we compared the mean error in between model and exper-
147 iment data for the following parameters: vertical COM amplitude a , swing/stance
148 ratio, walking speed v , virtual pivot point (VPP) length factor γ , COP speed and
149 distance (D_{COP}) travelled as shown in Fig. 6. We use the following equations from
150 existing literature for experimental walking.

$$a = 0.054v + 0.002 \quad [18] \quad (7)$$

$$v = (c)(s_l) \quad [18] \quad (8)$$

$$L_{VPP} = \gamma L \quad [18] \quad (9)$$

$$D_{COP} = 0.152h \quad [23] \quad (10)$$

151 where c is cadence, s_l is step length, L_{VPP} is distance between COM and virtual
152 pivot point, γ is the VPP factor usually around 1.8, D_{COP} is distance travelled
153 by the COP during stance and h is the height of the human. Winter et al. [23]

154 provided measures of ratios of different body parts with respect to human height.
155 Such a ratio for foot measure is shown in eq.(10). Swing/stance ratio is calculated
156 by dividing the swing time of a particular leg by its stance time during a gait
157 cycle. To compare the models with experiment data of adults we dimensionalize
158 the parameters. Walking speed is dimensionalized by multiplying \dot{x} with $\sqrt{gl_o}$,
159 where $l_o=1\text{m}$ is the uncompressed leg length. In Fig. 5, we compared solutions
160 at every apex y_i at \dot{x}_i 0.335 and $\theta_o = 76.33^\circ$. In Fig. 6 we calculate the average
161 of all limit cycle solutions for all dimensionalized apex speeds to make model-
162 experiment comparison.

163 One of the objectives of our study was to see if the relation among TD angle,
164 walking speed and COP speed provides steady state solutions for the given adult
165 speed range². We get steady state solutions for very slow to slow walking speeds
166 for SLIP and very slow to very fast walking speeds for SLIP_{COP}. For SLIP_{COP}
167 with both μ values, we see a larger error for COM amplitude and swing/stance
168 ratio at very slow to normal walking speeds, compared to SLIP. But the error
169 decreases as the walking speed increases. SLIP estimates COM amplitude much

²We classify walking speeds as very slow (0.7-1.12 m/s), slow (1.12-1.31 m/s), normal (1.31-1.58 m/s), fast (1.58-1.76 m/s) and very fast (1.76-2.19 m/s) based on the classification provided by [24].

170 better than $SLIP_{COP}$ at lower speed ranges because its optimized spring stiffness
171 values lie close to human leg stiffness. Fig. 6b illustrates the error of swing/stance
172 ratio. At lower walking speed, both models perform similarly. As walking speed
173 increases, the errors for both models decrease. At the normal walking speeds SLIP
174 provides less error than $SLIP_{COP}$; at 1.36 m/s, 25.72% error for SLIP, 55.17% for
175 $SLIP_{COP}$ ($\mu = 0$), and 61.13% for $SLIP_{COP}$ ($\mu = 1$). For higher walking speeds,
176 $SLIP_{COP}$ outperforms (error below 25%) SLIP, which fails to find a solution.

177 The concept of virtual pivot point (VPP) is illustrated in Fig. 3 and expressed
178 in eq.(9). In Fig. 6d the VPP factor (γ) is compared with the physiologically
179 measured value of 1.8 provided by [18]. As expected, SLIP model provides γ
180 which is equal to 1 under all scenarios because of its fixed pivot. $SLIP_{COP}$ ($\mu =$
181 0, 1) provides more accurate estimates of γ with approximately 20% error. VPP
182 is a good metric to measure the effectiveness of our COP progression model. The
183 error remains constant at 20% for most of the speed range but decreases to 10% at
184 very fast speed ran (see Fig. 6e). D_{COP} is calculated, for an adult with an average
185 height of 1.7 meters [11] with an uncompressed leg length, $L_o = 1m$. In Fig. 6f
186 we observe, $SLIP_{COP}$ shows quite a low error except at very slow and very fast
187 walking speeds: the least error of 4% at 0.75 m/s with $\mu = 1$ and 7% at 1.4m/s
188 with $\mu = 0$.

189 **4 Discussion**

190 Through this study we compared the effect of adding a translating COP to the
191 conventional SLIP model. The motivation behind using a translating COP was to
192 simulate the effects of the heel-to-toe pivoting of the foot during stance phase in
193 human walking. One of the objectives of our study was to improve the predictive
194 capabilities of SLIP for a wider speed range² when comparing with experimental
195 data. Utilizing experimental data (of the relation among walking speed, TD angle,
196 and COP speed) enables us to obtain limit cycle solutions at these speed ranges.
197 The relation between TD angle and walking speed also suggests that as the walk-
198 ing speed approaches 0, TD angle approaches 90 degrees (erect standing), which
199 can be considered as decent validation of our walking speed and TD angle rela-
200 tion. This shows that as the walking speed approaches a lower value step length
201 approaches 0. Lipfert et al. [11] showed that to obtain similar walking dynamics
202 at a given walking speed, the SLIP model was simulated at a steeper angle be-
203 cause of premature lift off at the correct TD angle. With the relation between TD
204 angle and walking this limitation is overcome. On the other hand, provision of
205 COP speed-walking speed relation leads to increase in stance time. When com-
206 paring the 2 models at similar optimized state variables, we see an increase in gait
207 distance for $SLIP_{COP}$ because of increase in its stance time. To comment upon

208 gait distance estimation of the 2 models we dimensionalize the result in Fig. 4c
209 with a leg length $L_o = 1m$ and speed of 1m/s so as to compare to a previous
210 model-experiment study using SLIP [11]. Upon comparing, the COM trajectories
211 in Fig. 4c, we observe that $SLIP_{COP}$ estimates the gait distance with an error of
212 0.05 m and SLIP with an error of 0.25 m [11]. One of the reasons for this un-
213 derestimation by SLIP could be its fixed pivot point. Although we used constant
214 stiffness in our models, we preferred optimizing the spring stiffness rather than
215 using predefined leg stiffness [11]. This was done because the relation among TD
216 angle, walking speed, and COP speed could affect the optimal value of stiffness.
217 We understand that the human walking gait is a consequence of the stabilization
218 occurring at the foot. This has led us to put more emphasis on the relation among
219 TD angle, walking speed, and COP speed rather than on leg stiffness as done by
220 Lipfert and colleagues. Although human muscular strength determines the flex-
221 ion and extension of our lower limbs during walking, it is difficult to measure this
222 strength just by observation. Through inverse dynamics we can utilize observable
223 kinematic and dynamic characteristics to understand more about the functioning
224 of human walking. The COP speed trajectory for the accelerated COP modality
225 shows a similar trend in COP speed as shown in the study by Cornwall and col-
226 leagues [25], with high speed at initial contact phase, lower speed at mid stance

227 and higher speed at TD. This U-shape speed profile correlates with the horizontal
228 COM acceleration F_x because COM decelerates in the first half of stance phase
229 and then accelerates in the next half. This suggests that our weighted function
230 approximates the acceleration of the COP quite well.

231 In Fig. 4a & c we see the effects of a translating COP which leads to higher
232 variation in vertical GRF and COM amplitude respectively, compared to SLIP.
233 Such behavior was also observed in the IP model [17] and POFT model [16],
234 where the addition of a translating COP increases the vertical displacement signif-
235 icantly. Bullimore et al. [16] also mention that due to a translating COP the stance
236 time for a leg increases which we also observe in $SLIP_{COP}$. They also mentioned
237 that addition of a COP progression model decreases the spring stiffness of the
238 model. The decrease in spring stiffness can be explained by eqns.(11)(12)(13). In
239 Fig. 4a, F_y at mid stance (apex) is lower for $SLIP_{COP}$ than SLIP. At apex the COM
240 experiences centripetal acceleration due to its weight and spring force. Hence,
241 upon referring Fig. 2, 3 and Table 2, the force balance for SLIP and $SLIP_{COP}$ at
242 apex is

$$m \frac{\dot{x}_{id}^2}{y_i} = k(L_o - y_{id}) - mg \quad (11)$$

$$m \frac{\dot{x}_{id}^2}{L_{VPP}} = k_{VPP}(L_o - y_{id}) - mg \quad (12)$$

Subtracting eqns.(12) from (11) we get,

$$m \frac{\dot{x}_{id}^2}{y_i} - m \frac{\dot{x}_{id}^2}{L_{VPP}} = k(L_o - y_{id}) - k_{VPP}(L_o - y_{id}) \quad (13)$$

243 As both sides of the eqn.(13) are positive with $y_i < L_{VPP}$, this implies $k > k_{VPP}$.

244 To reduce the vertical displacement occurring due to reduced spring stiffness,

245 Bullimore et al. [16] added a constraint on the vertical movement of the COM.

246 Constraining the vertical displacement for our models resulted a difficulty to find

247 limit cycle solutions and hence we relaxed this constraint. Lee et al. [17] showed

248 that with increasing walking speeds the error in COM vertical displacement in-

249 creases when compared to experimental data. We observe a decrease in error for

250 COM vertical displacement, at $\mu = 0$ and 1, with increasing walking speeds which

251 shows the effectiveness of our bipedal model. The IP model in the above studies

252 was simulated only for single stance which could have limited its predictive nature

253 unlike the SLIP and SLIP_{COP}.

254 One of the characteristics of walking is the relation between cadence and

255 step length represented by eqn.(8). We obtain quite low errors for both mod-

256 els for walking speed using eqn.(8) as seen in Fig. 6c. We observe an increase

257 in step length and decrease in cadence for SLIP_{COP} which was expected in our

258 study. With COP progression the distance between consecutive heel strikes in-

259 creases subsequently increasing the step length. This in turn reduces cadence (re-

260 fer eqn.(8)). As discussed before, due to COP progression we have an increase in
261 stance time which is also responsible for decrease in cadence because is defined as
262 steps per min. One more factor that is characteristic of a progressive COP model
263 is the generation of a virtual pivot point as discussed above (Fig. 3). To the best
264 of our knowledge, there exists no study with SLIP model that has estimated the
265 VPP factor γ . The average γ value with our proposed $SLIP_{COP}$ is around 1.4 with
266 a 20% mean error, where the range of γ is between 1.33 and 2.1. To put the value
267 of γ into perspective, we evaluate the distance travelled by the COP during stance.
268 As COP travels approximately a foot length [12], we evaluated the COP distance
269 D_{COP} for our speed range. The accelerated COP modality shows a considerably
270 lower error values than the constant velocity modality for very slow to normal
271 walking speeds. One of our objectives was to differentiate between the two COP
272 modalities $\mu = 0$ and 1. With D_{COP} we see that for very slow to slow speeds $\mu = 1$
273 provides better estimation and for normal walking speeds $\mu = 0$ is better. Overall
274 the accelerated model shows lower error value for D_{COP} for majority of speeds
275 suggesting its reliability over the constant velocity modality.

276 We propose a bipedal spring mass model utilizing the COP translation ob-
277 served during human walking. We compare this model with the SLIP model with
278 respect to human walking data. We observe that the SLIP and $SLIP_{COP}$ show

279 pretty high error estimates for COM vertical amplitude and swing/stance ratio at
280 very slow to slow walking speeds. At normal to very fast walking speeds, we see
281 the benefits of the $SLIP_{COP}$ as it not only provides limit cycle solutions for these
282 speed zones but also considerably decreases error in predicting COM amplitude
283 and swing/stance duration ratio. $SLIP_{COP}$ is able to reproduce a symmetrical COP
284 speed profile in the fore-aft direction. The distance traveled by the COP for the
285 two COP progression modes at normal walking speeds concurs with distance trav-
286 eled by the COP during human walking and can be considered as a substitute for
287 an ankle based walking model. This pilot study on using a translating COP based
288 SLIP model takes into consideration the fact that COP movement is closely related
289 to the GRF force in the horizontal direction.

290 In the future work, this model can be further developed by utilizing actual COP
291 data from human walking, which could enhance our models capabilities from the
292 point of view of simulating slow to normal walking speeds. This study will be
293 also undertaken from the point of view of assessing gaits in people with move-
294 ment disorder such as Cerebral Palsy, Stroke and Parkinson's. People with such
295 movement disorders often portray unequal strength in their legs. This affects their
296 walking style, foot placement consequently affecting their COP dynamics. De-
297 veloping our COP model towards adapting it to assess these movement disorders

298 would help us understand the difference between healthy and impaired walking

299 styles.

300 **List of abbreviations**

Abbreviations

GRF Ground reaction force

SLIP Spring loaded inverted pendulum

COM Center of mass

COP Center of pressure

TD Touch down

IP Inverted pendulum

POFT Point of force translation

LO Lift off

VPP Virtual pivot point

301 **Acknowledgements**

302 We would like to thank Dr. Leif Johannsen and Dr. Ing. Matteo Saveriano for

303 their inputs to our research.

304 **Competing interests**

305 We declare that this manuscript is original and has not been published before. We
306 know of no conflict of interest associated with this publication.

307 **Author contributions**

308 Karna Potwar conducted the research, dealing with generating the hypothesis as
309 well as simulating and analyzing the bipedal walking model. He also documented
310 and edited the manuscript. Dongheui Lee supervised this research and critiqued
311 the manuscript.

312 **Funding**

313 This work was funded by the German Academic Exchange Service (DAAD),
314 TUM International Graduate School of Science & Engineering and Helmholtz
315 Association.

316 **References**

- 317 [1] R. J. Full and D. E. Koditschek, “Templates and anchors: neuromechanical
318 hypotheses of legged locomotion on land,” *Journal of experimental biology*,
319 vol. 202, no. 23, pp. 3325–3332, 1999.
- 320 [2] R. M. Alexander, “Mechanics of bipedal locomotion,” in *Zoology*. Elsevier,
321 1976, pp. 493–504.
- 322 [3] S. Mochon and T. A. McMahon, “Ballistic walking,” *Journal of biomechan-*
323 *ics*, vol. 13, no. 1, pp. 49–57, 1980.
- 324 [4] R. Blickhan, “The spring-mass model for running and hopping,” *Journal of*
325 *biomechanics*, vol. 22, no. 11-12, pp. 1217–1227, 1989.
- 326 [5] T. A. McMahon and G. C. Cheng, “The mechanics of running: how does
327 stiffness couple with speed?” *Journal of biomechanics*, vol. 23, pp. 65–78,
328 1990.
- 329 [6] S. Siegler, R. Seliktar, and W. Hyman, “Simulation of human gait with the
330 aid of a simple mechanical model,” *Journal of biomechanics*, vol. 15, no. 6,
331 pp. 415–425, 1982.

- 332 [7] M. Van Gorp, H. Schamhardt, and A. Crowe, “The ground reaction force
333 pattern from the hindlimb of the horse simulated by a spring model,” *Cells
334 Tissues Organs*, vol. 129, no. 1, pp. 31–33, 1987.
- 335 [8] M. G. Pandy, “Simple and complex models for studying muscle function
336 in walking,” *Philosophical Transactions of the Royal Society of London B:
337 Biological Sciences*, vol. 358, no. 1437, pp. 1501–1509, 2003.
- 338 [9] F. E. Zajac, R. R. Neptune, and S. A. Kautz, “Biomechanics and muscle
339 coordination of human walking: part ii: lessons from dynamical simulations
340 and clinical implications,” *Gait & posture*, vol. 17, no. 1, pp. 1–17, 2003.
- 341 [10] H. Geyer, A. Seyfarth, and R. Blickhan, “Compliant leg behaviour explains
342 basic dynamics of walking and running,” *Proceedings of the Royal Society
343 of London B: Biological Sciences*, vol. 273, no. 1603, pp. 2861–2867, 2006.
- 344 [11] S. W. Lipfert, M. Günther, D. Renjewski, S. Grimmer, and A. Seyfarth, “A
345 model-experiment comparison of system dynamics for human walking and
346 running,” *Journal of Theoretical Biology*, vol. 292, pp. 11–17, 2012.
- 347 [12] M.-C. Chiu, H.-C. Wu, and L.-Y. Chang, “Gait speed and gender effects
348 on center of pressure progression during normal walking,” *Gait & posture*,
349 vol. 37, no. 1, pp. 43–48, 2013.

- 350 [13] S. Fuchioka, A. Iwata, Y. Higuchi, M. Miyake, S. Kanda, and T. Nishiyama,
351 “The forward velocity of the center of pressure in the midfoot is a major pre-
352 dictor of gait speed in older adults,” *International Journal of Gerontology*,
353 vol. 9, no. 2, pp. 119–122, 2015.
- 354 [14] M. A. Sharbafi and A. Seyfarth, *Bioinspired Legged Locomotion: Models,*
355 *Concepts, Control and Applications.* Butterworth-Heinemann, 2017.
- 356 [15] D. Maykranz, S. Grimmer, S. Lipfert, and A. Seyfarth, “Foot function in
357 spring mass running,” in *Autonome Mobile Systeme.* Springer, 2009, pp.
358 81–88.
- 359 [16] S. R. Bullimore and J. F. Burn, “Consequences of forward translation of the
360 point of force application for the mechanics of running,” *Journal of theoret-*
361 *ical biology*, vol. 238, no. 1, pp. 211–219, 2006.
- 362 [17] C. R. Lee and C. T. Farley, “Determinants of the center of mass trajectory
363 in human walking and running.” *Journal of experimental biology*, vol. 201,
364 no. 21, pp. 2935–2944, 1998.
- 365 [18] S. Miff, S. A. Gard, and D. Childress, “The effect of step length, cadence,
366 and walking speed on the trunk’s vertical excursion,” in *Proceedings of the*
367 *22nd Annual International Conference of the IEEE Engineering in Medicine*

368 *and Biology Society (Cat. No. 00CH37143)*, vol. 1. IEEE, 2000, pp. 155–
369 158.

370 [19] R. Alexander, “Optimization and gaits in the locomotion of vertebrates,”
371 *Physiological reviews*, vol. 69, no. 4, pp. 1199–1227, 1989.

372 [20] S. Shen and J. Seipel, “Effective leg stiffness of animal running and the co-
373 optimization of energetic cost and stability,” *Journal of theoretical biology*,
374 vol. 451, pp. 57–66, 2018.

375 [21] Z. Shen and J. Seipel, “A fundamental mechanism of legged locomotion with
376 hip torque and leg damping,” *Bioinspiration & biomimetics*, vol. 7, no. 4, p.
377 046010, 2012.

378 [22] S. Strogatz, *Nonlinear dynamics and chaos: with application to physics,*
379 *biology, chemistry and engineering.* CRC press, 2018.

380 [23] D. A. Winter, *Biomechanics and motor control of human movement.* John
381 Wiley & Sons, 2009.

382 [24] R. Drillis, “Objective recording and biomechanics of pathological gait,” *An-*
383 *nals of the New York Academy of Sciences*, vol. 74, no. 1, pp. 86–109, 1958.

- 384 [25] M. W. Cornwall and T. G. McPoil, “Velocity of the center of pressure during
385 walking,” *Journal of the American Podiatric Medical Association*, vol. 90,
386 no. 7, pp. 334–338, 2000.

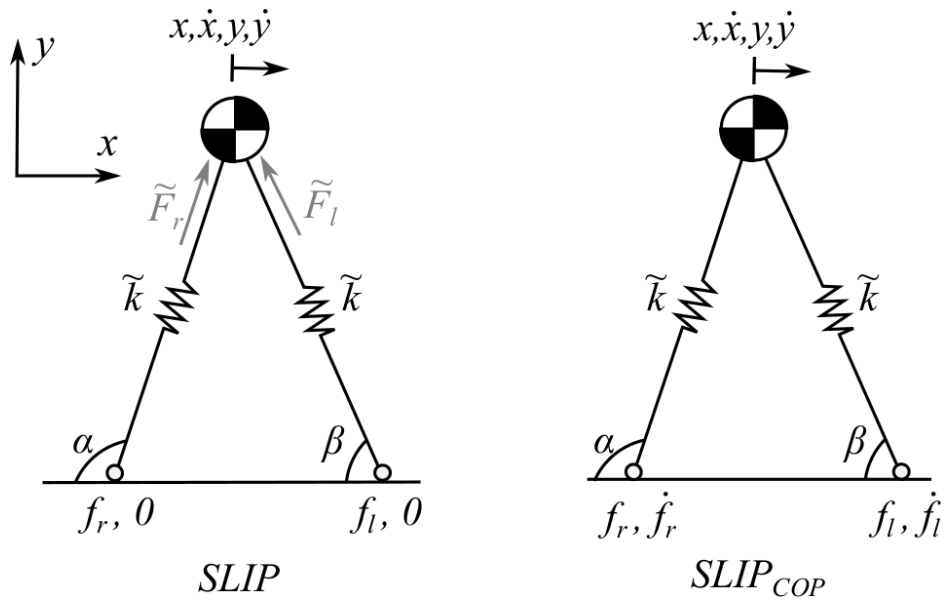


Figure 1: Diagram showing the two models, (Left) SLIP and (Right) SLIP with translating COP (SLIP_{COP}) with COM and COP coordinates in the sagittal plane.

Subscripts r and l stand for right and left leg respectively.

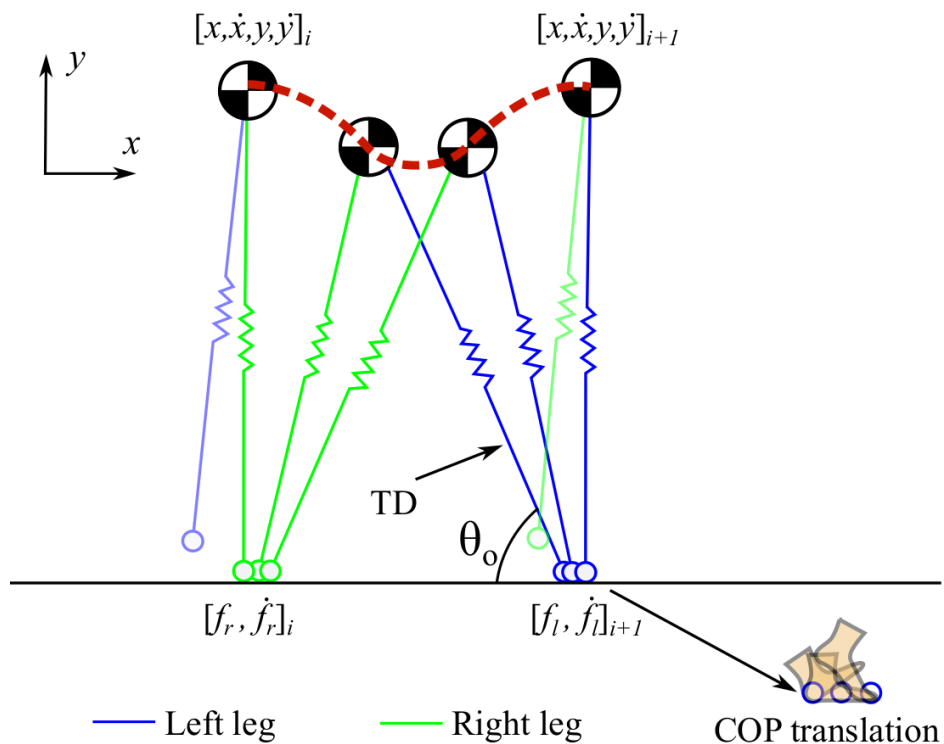


Figure 2: A limit cycle of the translating COP model. The model starts at the apex i and attains the consecutive apex $i + 1$, while the COP translates along the ground.

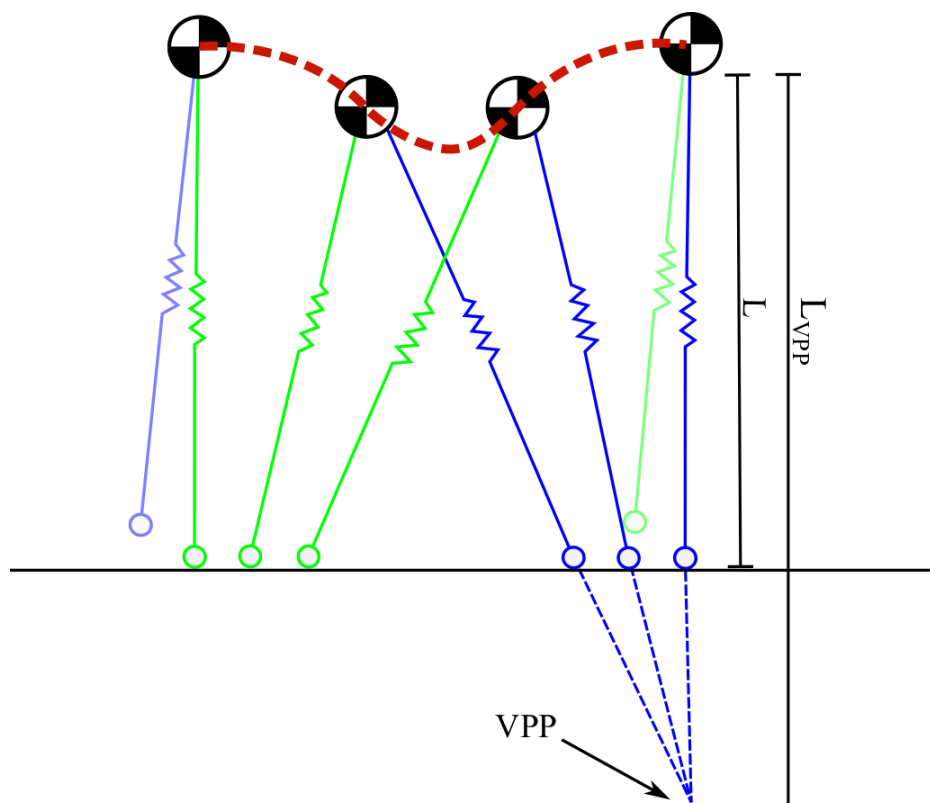


Figure 3: Translation of the COP in $SLIP_{COP}$ leads to a virtual pivot point (VPP) under the surface. l_v is the extended length where $l_v=1.8l$ [18] during walking .

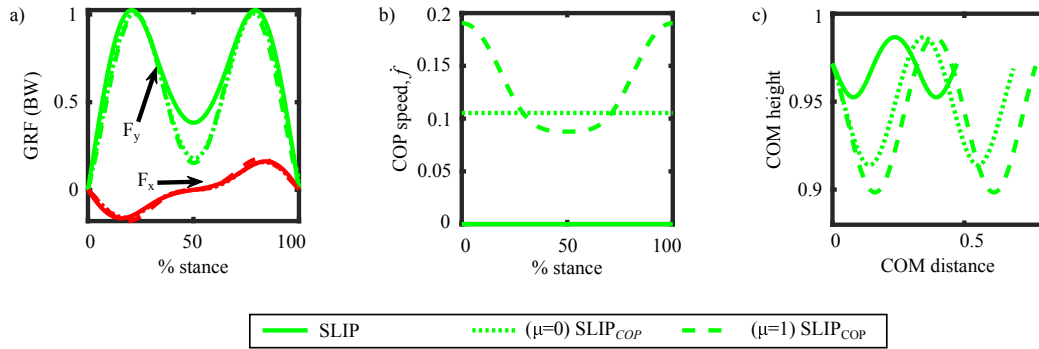


Figure 4: GRF, COP speed and COM trajectory plotted for SLIP and SLIP_{COP} ($\mu = 0$ and $\mu = 1$) with parameters in Table 1.

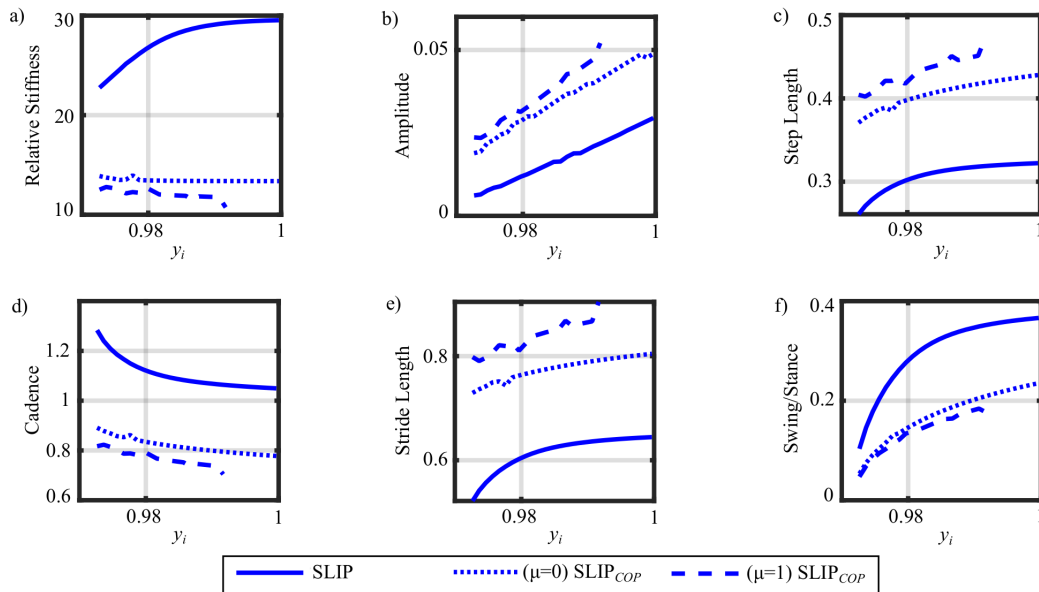


Figure 5: Plotting temporal and distance variables for different values of y_i as at an apex speed \dot{x}_i of 0.335 and θ_o of 76.33° .

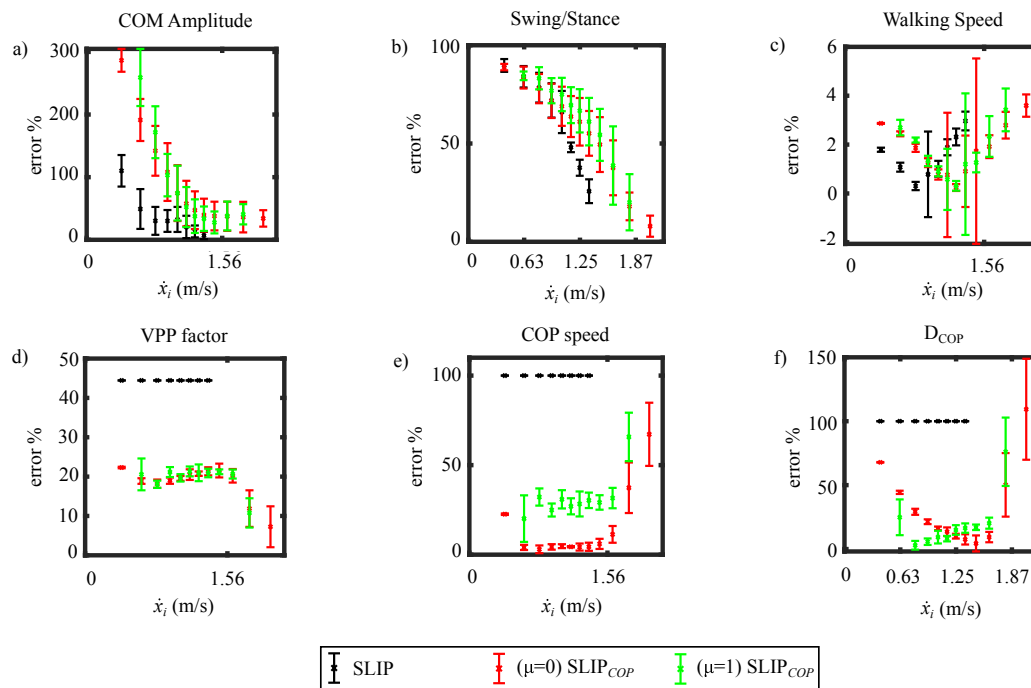


Figure 6: Mean errors of the obtained model parameters (amplitude, swing/stance duration ratio, average walking speed, VPP factor, average COP speed and COP distance) with respect to experimental human data.

Parameters	SLIP	SLIP _{COP}	
		$\mu = 0$	$\mu = 1$
\dot{x}_i	0.335	0.335	0.335
y_i	0.986	0.986	0.986
θ_o	76.33	76.33	76.33
\dot{f}_i	0	0.105	0.087
\tilde{k}	28.67	13.39	11.48

Table 1: Simulation parameters for results in Figure 5. $x_i = \dot{y}_i = 0$

Fitted Parameter	Equation
Touchdown angle, θ_o	$\theta_o = 0.36\dot{x}_i^3 + 0.25\dot{x}_i^2 - 0.84\dot{x}_i + 1.57$
COP velocity lower bound, \dot{f}_{LB}	$\dot{f}_{LB} = 0.21\dot{x} - 0.002$
COP velocity upper bound, \dot{f}_{UB}	$\dot{f}_{UB} = 0.74\dot{x} + 0.22$

Table 2: Parameter relations obtained from physiological data[11, 12]. Subscript

LB and *UB* stand for lower bound and upper bound respectively.